

specific expression of the *lbc₃* promoter in the distantly related legume *L. corniculatus* has further implications concerning the control of nodule expressed genes. *Lotus corniculatus* belongs phylogenetically to the tribe Loteae while soybean belongs to the Phaseoleae⁴². The microsymbiont *Rhizobium loti* is a species separate from the soybean symbiont *B. japonicum*¹ and nodulates plants from a different cross-inoculation group. It appears therefore that both a putative bacterial induction signal and DNA sequences involved in nodule-specific expression of plant 'nodulin' genes are conserved in the legume *Rhizobium* sym-

Received 5 February; accepted 15 April 1986.

1. Vincent, J. M. in *The Biology of Nitrogen Fixation* (ed. Quispel, A.) 265–341 (North-Holland, Amsterdam, 1974).
2. Vincent, J. M. in *Nitrogen Fixation II* (eds Newton, W. E. & Orme Johnson, W. H.) 103–129 (University Park, Baltimore, 1980).
3. Legocki, R. P. & Verma, D. P. S. *Cell* **20**, 153–163 (1980).
4. Bisseling, T., Been, C., Klugkist, J., Van Kammen, A. & Nadler, K. *EMBO J.* **2**, 961–966 (1983).
5. Cullimore, J. V. et al. *J. molec. appl. Genet.* **2**, 589–599 (1984).
6. Joachimsen, B. & Rasmussen, O. in *Abstr. 1st int. Symp. Molecular Genetics of the Bacteria-Plant Interactions*, 83 (Springer, Berlin, 1982).
7. Nguyen, T., Zelechowska, M., Foster, V., Bergmann, H. & Verma, D. P. S. *Proc. natn. Acad. Sci. U.S.A.* **82**, 5040–5044 (1985).
8. Fuchsman, W. H. & Appleby, C. A. *Biochim. biophys. Acta* **579**, 314–324 (1979).
9. Bojsen, K., Abildsten, D., Jensen, E. Ø., Paludan, K. & Marcker, K. A. *EMBO J.* **2**, 1165–1168 (1983).
10. Lee, J. S., Brown, G. G. & Verma, D. P. S. *Nucleic Acids Res.* **11**, 5541–5553 (1983).
11. Marcker, A., Lund, M., Jensen, E. Ø. & Marcker, K. A. *EMBO J.* **3**, 1691–1695 (1984).
12. Grosfeld, G. C., de Boer, E., Shewmaker, C. K. & Flavell, R. A. *Nature* **295**, 120–126 (1982).
13. Dierks, P. et al. *Cell* **32**, 695–706 (1983).
14. Wright, S., Rosenthal, A., Flavel, R. & Grosfeld, F. *Cell* **38**, 265–273 (1984).
15. Leemans, J. et al. *J. molec. appl. Genet.* **1**, 149–164 (1981).
16. Van Haute, E. et al. *EMBO J.* **3**, 411–417 (1983).
17. White, F. F. & Nester, E. W. *J. Bact.* **141**, 1134–1141 (1980).
18. Chilton, M.-D. et al. *Nature* **295**, 432–434 (1982).
19. Pankhurst, C. E. *Can. J. Microbiol.* **23**, 1026–1033 (1977).
20. Viborg, O. et al. *EMBO J.* **4**, 755–759 (1985).
21. Gausling, K. & Barkardottir, R. *Eur. J. Biochem.* (in the press).
22. Brissian, N. & Verma, D. P. S. *Proc. natn. Acad. Sci. U.S.A.* **79**, 4055–4059 (1982).
23. Nienhuis, A. W. & Benz, E. J. *New Engl. J. Med.* **297**, 1318–1328; 1371–1381, 1430–1436 (1977).
24. Marton, L., Wullems, G. J., Molendijk, L. & Schilperoort, R. A. *Nature* **277**, 129–131 (1979).
25. Horsch, R. B. et al. *Science* **227**, 1229–1231 (1985).
26. Pollock, K., Barfield, D. G., Robinson, S. J. & Shields, R. *Pl. Cell Rep.* **4**, 202–205 (1985).
27. Zambryski, P. et al. *EMBO J.* **2**, 2143–2150 (1983).
28. Herrera-Estrella, L. et al. *EMBO J.* **2**, 987–995 (1983).
29. De Block, M., Herrera-Estrella, L., Van Montagu, M., Schell, J. & Zambryski, P. *EMBO J.* **3**, 1681–1689 (1984).
30. Sengupta-Gopalan, C., Reichert, N. A., Barker, R. F., Hall, T. L. & Kemp, J. O. *Proc. natn. Acad. Sci. U.S.A.* **82**, 3320–3324 (1985).
31. Lampka, G., Nagy, F. & Chua, N.-H. *Nature* **316**, 750–752 (1985).
32. De Block, M., Schell, J. & Van Montagu, M. *EMBO J.* **4**, 1367–1372 (1985).
33. Simpson, J. et al. *EMBO J.* **4**, 2723–2729 (1985).
34. Nagy, F., Morelli, G., Graley, S. G. & Chua, N.-H. *EMBO J.* **4**, 3063–3068 (1985).
35. Beachy, R. N. et al. *EMBO J.* **4**, 3047–3053 (1985).
36. Jones, J. D. G., Dunsmuir, P. & Bedbrook, J. *EMBO J.* **4**, 2411–2418 (1985).
37. Jensen, E. Ø., Marcker, K. A. & Villadsen, I. S. *EMBO J.* **5** (in the press).
38. Herrera-Estrella, L. et al. *Nature* **310**, 115–120 (1984).
39. Morelli, G., Nagy, F., Fraley, R. T., Rogers, S. G. & Chua, N.-H. *Nature* **315**, 200–204 (1985).
40. Facciotti, D., O'Neal, J. K., Lee, S. & Shewmaker, C. H. *Biotechnology* **3**, 241–246 (1985).
41. Timko, M. P. et al. *Nature* **318**, 579–582 (1985).
42. Polhill, R. M. in *Advances in Legume Systematics* Vol. 1 (eds Polhill, R. M. & Raven, D. H.) (University of Reading, 1981).
43. Trinick, M. J. *J. appl. Bact.* **49**, 39–53 (1980).
44. Daheze, P., De Greve, H., Decraemer, H., Schell, J. & Van Montagu, M. *Nucleic Acids Res.* **7**, 1837–1849 (1979).
45. Pomploni, M., Spano, L., Sabbadini, M. G. & Costantino, P. *Plasmid* **10**, 119–129 (1983).
46. Dellaporta, S. L., Wood, J. B. *Pl. molec. Biol.* **1**, 10–21 (1983).
47. Boel, E. et al. *Proc. natn. Acad. Sci. U.S.A.* **80**, 2866–2869 (1983).

Fluorescence detection in automated DNA sequence analysis

Lloyd M. Smith, Jane Z. Sanders, Robert J. Kaiser, Peter Hughes, Chris Dodd, Charles R. Connell*, Cheryl Heiner*, Stephen B. H. Kent & Leroy E. Hood

Division of Biology, California Institute of Technology, Pasadena, California 91125, USA

* Applied Biosystems, Inc., Foster City, California 94404, USA

We have developed a method for the partial automation of DNA sequence analysis. Fluorescence detection of the DNA fragments is accomplished by means of a fluorophore covalently attached to the oligonucleotide primer used in enzymatic DNA sequence analysis. A different coloured fluorophore is used for each of the reactions specific for the bases A, C, G and T. The reaction mixtures are combined and co-electrophoresed down a single polyacrylamide gel tube, the separated fluorescent bands of DNA are detected near the bottom of the tube, and the sequence information is acquired directly by computer.

THE structural analysis of DNA has an increasingly important role in modern molecular biology. About 4×10^6 bases of DNA have been sequenced since the introduction of the enzymatic method of rapid sequencing developed by Sanger and co-workers^{1,2} and the chemical method developed by Maxam and Gilbert³. Typically, four separate reactions are performed on the particular DNA segment to be analysed. In the enzymatic method, these reactions produce DNA fragments terminating in either adenosine (A), cytosine (C), guanosine (G) or thymidine (T). In the chemical method fragments terminating in G, G+A, C+T, or C are typically produced. In both cases the four sets of reaction products are electrophoresed in adjacent lanes of a high-resolution polyacrylamide gel. An autoradiographic image of the gel is produced which can be examined

to determine the relative lengths of the DNA fragments generated in each of the four reactions. The DNA sequence is inferred directly from this information. Both these techniques are highly effective but are also very labour-intensive, fairly expensive and involve the use of radioisotopes. For these reasons, and because many genes remain to be sequenced (there are 3×10^9 bases in the human genome alone), we have undertaken the development of an automated and non-isotopic method of DNA sequence analysis.

Strategy

Our approach has two major aims. The first is to acquire, store and analyse sequence information directly by computer. Doing this in real-time during the gel electrophoresis eliminates the

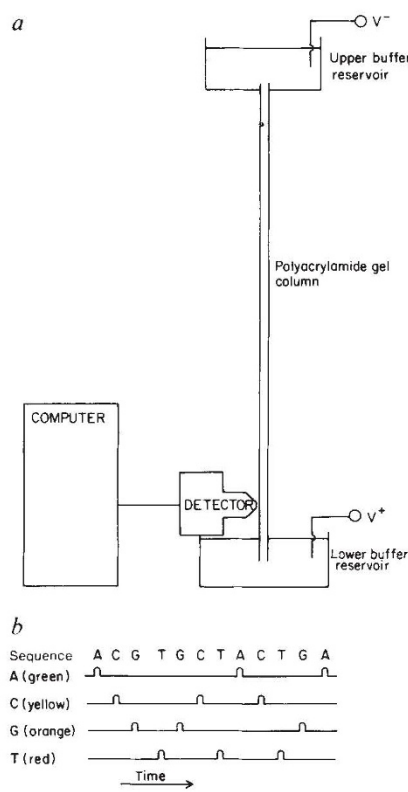


Fig. 1 *a*, Simplified diagram of the automated DNA sequenator. *b*, Idealized output from the automated DNA sequenator.

transfer of information from gel to film (autoradiography), the tedious manual analysis and the need to run several overlapping gels; instead, a single gel can be run for as long as resolvable sequence is obtained. The second aim is to avoid the use of radioisotopes, which are hazardous, costly and unstable.

With these considerations in mind, we have developed a strategy for the automated sequence analysis of DNA which is based on two key points (proposed initially in ref. 4). First, fluorophores are used for detection rather than radioisotopes. Fluorescence provides sufficient sensitivity for real-time optical detection of the small amounts of DNA present in DNA sequencing gels ($\sim 10^{-15}$ mol per band) (see the discussion below). Second, four different fluorophores are used, one for each of the base-specific reactions. The reaction products are combined and co-electrophoresed, and the DNA fragments generated in each reaction are detected near the bottom of the gel and identified by their colour. These fluorescence data are continuously acquired and stored by computer during the electrophoresis. The data may then be analysed by computer to yield the DNA sequence. An idealized version of this process is depicted in Fig. 1.

We applied this strategy to Sanger's enzymatic method of DNA sequence analysis. We use chemically synthesized fluorescent oligonucleotide primers to label the DNA fragments. When these fluorescent primers are used instead of the usual underivatized primer in the enzymatic sequencing reactions, the DNA fragments generated in the reactions are fluorescent.

Chemistry

The first step in implementing this strategy was to develop chemistry for the synthesis of the fluorescent oligonucleotide primers^{4,5}. Briefly, we synthesized a derivative of thymidine which contains a phosphoramidite moiety at the 3' carbon and a protected amino group at the 5' carbon. When this molecule is used in the final addition cycle of oligonucleotide synthesis by the phosphoramidite method (see ref. 6 for review), the product after deprotection and cleavage from the solid phase is an oligonucleotide containing a single aliphatic amino group

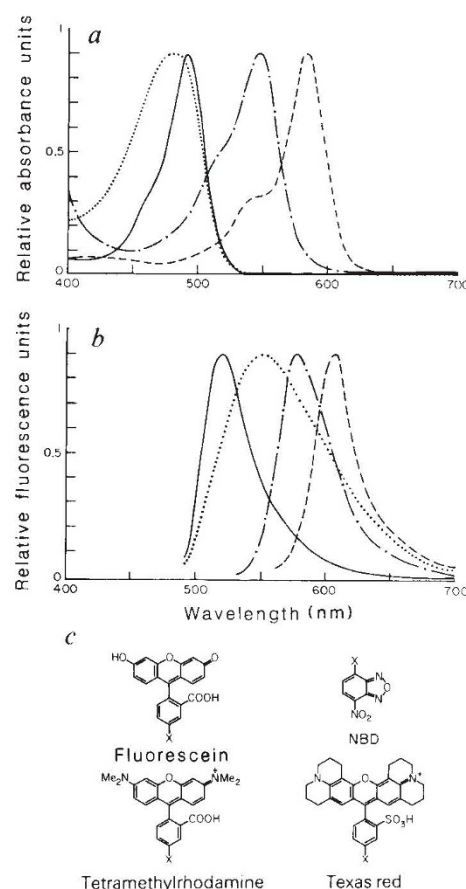


Fig. 2 *a*, Absorption spectra of the four dyes used in the DNA sequenator: —, fluorescein; ···, NBD; -·-, tetramethylrhodamine; -·-·-, Texas Red. *b*, Fluorescence emission spectra of the four dyes; the same line types as in *a*, are used to denote the dyes. *c*, Chemical structures of the four dyes. X, The moiety to which the dye is bound, for example, an oligonucleotide primer. **Methods.** All spectra were obtained in 10 mM sodium carbonate buffer, pH 9.0; absorption spectra were taken on an H/P 8451 spectrophotometer; fluorescence spectra were taken on a Perkin-Elmer MPF4 spectrofluorimeter (uncorrected). The following dye derivatives were used for measurements: fluorescein isothiocyanate (FITC), NBD aminohexanoic acid, Texas Red (all from Molecular Probes, Junction City, Oregon); and tetramethylrhodamine isothiocyanate (Research Organics, Inc., Cleveland, Ohio).

at the 5' terminus. This material may then be conjugated readily to any of various commercially available amino-reactive fluorescent dyes to yield the corresponding oligonucleotide derivative.

The selection of a set of four fluorophores was central to development of the DNA sequenator. Several criteria were used in the selection of these fluorophores. (1) The absorption and emission maxima had to be in the visible region of the spectrum, as far to the red end as possible, to minimize scattering and fluorescence background. (2) To be able to distinguish between the dyes effectively, their emission maxima had to be well resolved from one another. (3) The dyes had to be highly fluorescent to provide sufficient detection sensitivity. (4) The dyes should not significantly impair the hybridization of the oligonucleotide primer, as this would also decrease the efficiency of synthesis in the sequencing reactions. Finally, the electrophoretic mobility of the DNA fragments should not be distorted unacceptably by the presence of the dyes. The chemical structures and absorption and emission spectra of the four dyes we have chosen are shown in Fig. 2. Their absorption and emission maxima range from 486 nm (4-chloro-7-nitrobenzo-2-oxa-1-diazole (NBD) absorption maximum) to 604 nm (Texas Red emission maximum), well within the visible region of the spectrum. The emission maxima are evenly spaced at 30-nm

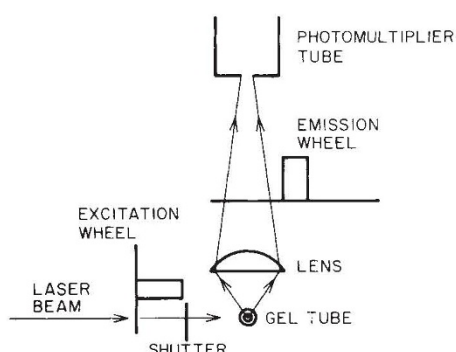


Fig. 3 Diagram of the optical configuration used for within-gel detection of fluorescence at four different wavelengths.

intervals, allowing reasonably good spectral discrimination. All the dyes have good fluorescence sensitivity, and are widely used and readily available. Conjugates of these dyes and an oligonucleotide primer (with the sequence 5' CCCAGTCACGACGTT 3', used in the single-stranded M13 phage vectors) were prepared and tested in conventional sequencing reactions using radioisotope detection (see ref. 4 for details). All the dye-primer conjugates were effective in the DNA sequencing reactions. The dyes do, however, affect the electrophoretic mobility of the DNA fragments to which they are bound; this necessitates a mobility correction to the sequence data which is discussed in the section on data analysis. The suitability of these primers in fluorescence-based detection was tested in instrumentation constructed for that purpose, as described below.

Instrumentation

The primary consideration in the design of the fluorescence detection apparatus was sensitivity. We performed preliminary experiments using radiolabelled nucleoside triphosphates of known specific activity to measure the amount of DNA present in a single band of a conventional sequencing gel, and obtained values of the order of 10^{-15} – 10^{-16} mol DNA per band. If the DNA is assumed to occupy a volume of 1 mm^3 , the DNA concentration is 10^{-9} – 10^{-10} M. Therefore, the instrument had to be capable of detecting dye concentrations of that order. This level of detection is readily achieved in commercial spectrophotometer systems. However, detection directly within the gel leads to much higher background scatter from the gel and from the circular glass tubing than is normally encountered, leading to decreased sensitivity. We therefore chose to use a laser excitation source in order to obtain maximum sensitivity, and have continued to use the laser source in subsequent work.

Figure 3 shows a schematic diagram of the optics used for detection of the fluorescent bands of DNA in the tube gel. The beam from an argon-ion laser (Lexel 65-0.1) operated in 'multi-line' mode is passed through a 1-nm-bandpass interference filter (to select out either the 488-nm or 514-nm laser line for excitation) mounted on a circular 'excitation' wheel and directed into a gel tube (glass or quartz tubing of 1–2 mm internal diameter; typically a 50-cm-long 8% polyacrylamide/6 M urea gel with the laser beam at 40 cm from the top of the gel) suspended between two tanks containing electrophoresis buffer. A single, fast-collection lens (Melles Griot 01 LAG 013, F/0.7) is used to collect the emitted light and focus it through a 10-nm-bandpass filter (Corion S10-x-R series, where x denotes the bandpass wavelength in nanometres, chosen to match the emission maximum of the dye being used) mounted on a second circular emission wheel, and onto the aperture of a photomultiplier tube (Hamamatsu R928). The optics are mounted on an optical table (MST46 with NN4-28 legs; Newport Research Corporation) enclosed in a dark room which has been painted black, and appropriate baffling is used to prevent stray light from reaching the photomultiplier tube. Four interference filters are mounted

at equally spaced intervals on each filter wheel, and a given excitation filter is always used in conjunction with a given emission filter. The filter pairs used are (in the order excitation filter, emission filter) 488, 520; 488, 550; 514, 580; 514, 610. The use of two different excitation wavelengths gives more efficient excitation of the different dyes (tetramethylrhodamine and Texas Red are excited more efficiently at 514 nm, whereas fluorescein and NBD are excited more efficiently at 488 nm) and thereby provides greater detection sensitivity. Neutral-density filters (Melles Griot BK-7 series) are also used in conjunction with the bandpass excitation filters to balance the baseline gel scatter levels obtained in each filter position. Light-emitting diodes and phototransistors are used to sense the position of the wheels. The excitation and emission wheels are accelerated and decelerated between the different filter positions using time intervals between pulses to the stepper motor that have been chosen to yield a constant acceleration. The movement of the wheel from one position to the next took 0.7 s, and the wheel was held stationary at each position for 0.8 s, giving a total time of 1.5 s between data points. A Uniblitz shutter (Vincent Associates) to protect the photomultiplier tube from excess scattered laser light was inserted into the laser beam and appropriate electronics were constructed to close the shutter if the photomultiplier tube (PMT) current exceeded a pre-set limit. Software was written to close the shutter, align both of the wheels into their starting positions, and then to re-open the shutter and commence data acquisition.

Typically, 8,000 points were taken for each of the four filter positions (total of 32,000 points) in a 13-h run; this rate of data acquisition gives 40 or more data points per DNA peak, under the electrophoretic conditions used. Filtering of the data to eliminate high-frequency noise was performed at three levels. First, an analog filter with a 100-ms time constant was used on the phototube output. Second, at each filter position, 200 data points were taken in succession and averaged, to yield a single point which was stored. At the 40-kHz rate of the Tecmar analog-to-digital converter, this required ~ 5 ms. Finally, the data were smoothed further with a low-pass Fourier filter included in the analysis (see below). Figure 4 shows a set of four-dye data obtained with this system. The raw data are shown in Fig. 4a; b and c show the same data after analysis. The procedures used in data analysis are described briefly below. These data demonstrate the practicality of this four-dye fluorescence approach for automated DNA sequence analysis.

Data analysis

If the raw data obtained with this instrument were as readily interpretable as the idealized data presented in Fig. 1b, very little data analysis would be required to determine the DNA sequence. In reality, however, several factors render the analysis of the data more complex. First, the emission spectra of the different dyes overlap substantially (see Fig. 2b); because of this, peaks corresponding to the presence of a single dye are seen in more than one channel. To discern the DNA sequence, one must therefore perform a multicomponent analysis to determine the different amounts of the four dyes present in the gel at any given time. The second major factor complicating the analysis is that the different dye molecules impart non-identical electrophoretic mobilities to the DNA fragments (see ref. 4). The fluorescein- and rhodamine-labelled DNA fragments move as if they were approximately one base longer than the NBD-labelled fragments, and the fragments labelled with Texas Red move as if they were approximately $1\frac{1}{4}$ bases longer. These mobility shifts must be compensated for. The third complicating factor in the analysis of the data comes from the imperfections of the enzymatic method of DNA sequence analysis itself. It is well known that the enzymatic method suffers from several anomalous traits, such as substantial variations in the intensity of bands in a given reaction, and occasional areas that prove difficult to sequence (thought to be associated with regions of

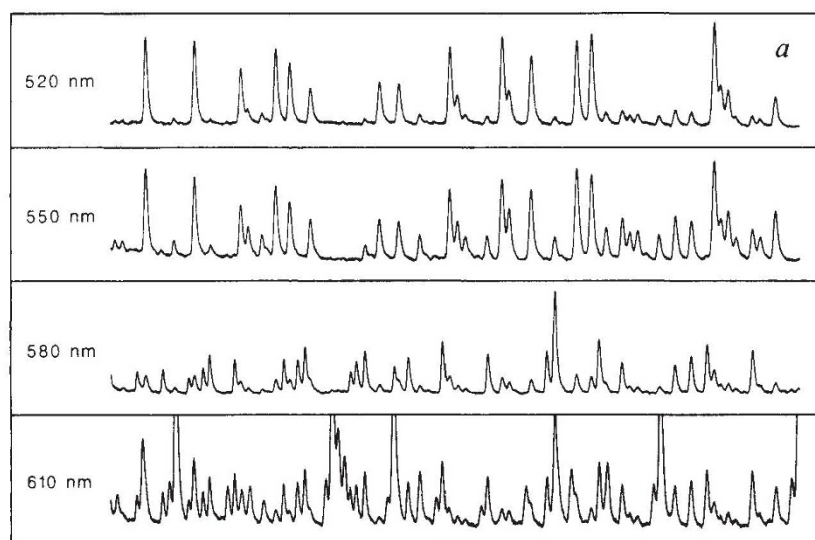
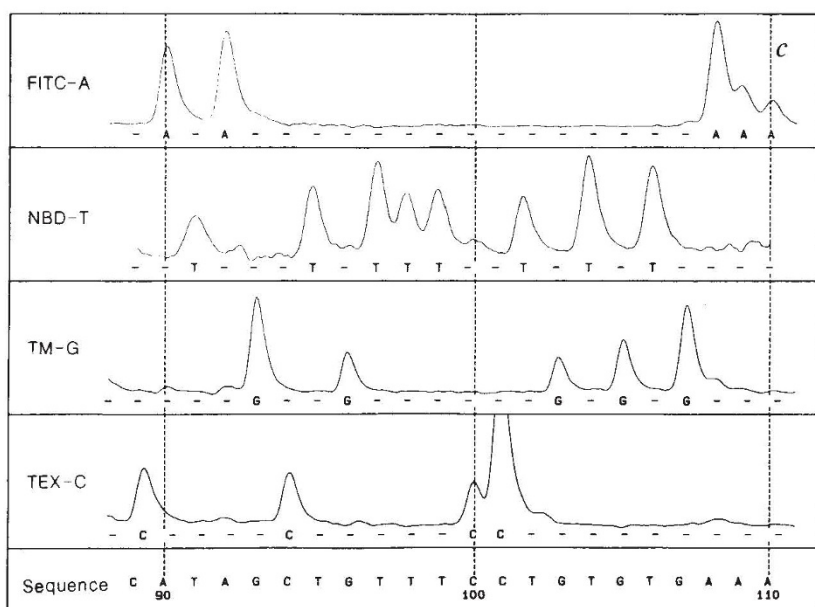
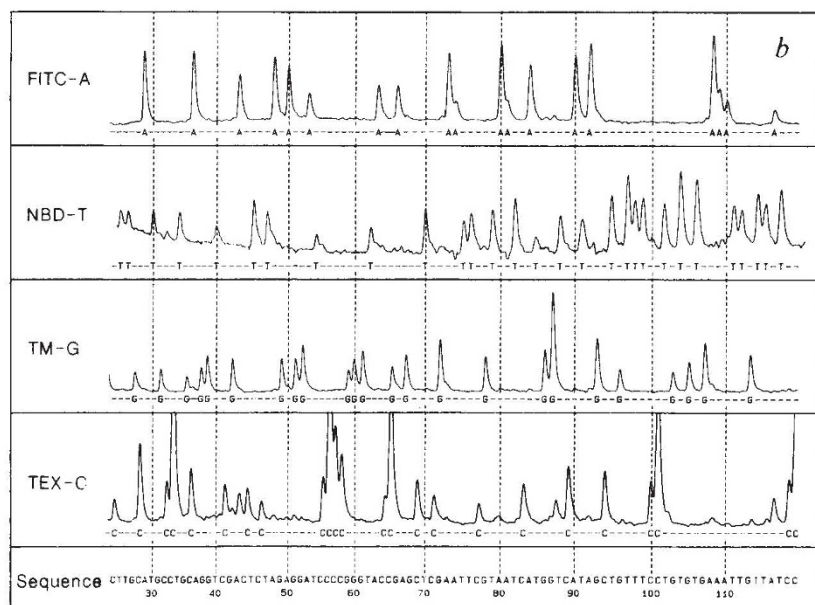


Fig. 4 Fluorescence data (*a*, raw; *b*, analysed) obtained from a mixture of four sequencing reactions. *c*, Expanded plot of 1,000 points of the analysed data. The mixture was applied to a single gel tube (quartz tubing with i.d. 1.3 mm; Heraeus Amersil, Sayreville, New Jersey) and detected using the optical configuration shown in Fig. 3 and described in the text. The relative amounts of each reaction used were chosen to give comparable signal intensities for each dye. This mixture contained 0.025 units of an FITC-A reaction, 0.1 units of Texas Red-C (Tex-C), 0.15 units of tetramethylrhodamine-G (TM-G), and 0.4 units of NBD-T, mixed with one volume of formamide, in a total volume of 14 μ l. A unit amount of sequencing reaction contains 0.4 pmol of template DNA and 0.8 pmol of primer DNA. The protocols used in the preparation and loading of the sequencing reactions are given in detail in ref. 6. See text for details of the data analysis.



secondary structure in the DNA itself). These complications must be handled in the analysis.

The procedures we have used in data analysis are described in detail in ref. 5. Briefly, the analysis consists of five steps: (1) High-frequency noise is removed by using a low-pass Fourier filter. (2) The time delay (1.5–4.5 s) between measurements at different wavelengths is partially corrected for by linear interpolation between successive measurements. (3) A multicomponent analysis is performed on each set of four data points; this computation yields the amount of each of the four dyes present in the detector as a function of time. (4) The peaks present in the data are located. (5) The mobility shift introduced by the dyes is corrected for using empirically determined correction factors. Figure 4b shows the processed data obtained when these five steps were applied to the raw data of Fig. 4a, and Fig. 4c shows an expanded plot of a region of 1,000 data points taken from Fig. 4b; the DNA sequence is aligned with the data. The correspondence between the sequence and the order of peaks obtained in the different channels is evident.

To date we have successfully executed hundreds of single-dye runs, 20–30 two-dye runs, and about 10 four-dye runs. In single-dye runs we often obtain well resolved and clearly discernible sequence beyond base 400 in ~16 h (data not shown). In four-dye runs we generally have obtained ~200 bases of clear sequence information. Present efforts are directed towards further defining and optimizing the parameters important in obtaining good resolution.

Sensitivity

The question is often raised of how the sensitivity of the fluorescence method compares with the sensitivity of conventional radioactive methods. The comparison is complicated by the fact that in the radioactive detection methods, the signal is integrated (by exposure on film) over long time periods ranging from hours to days. In contrast, the fluorescence approach uses real-time acquisition with integration times of a fraction of a second per data point; sensitivity is naturally much lower when the signal is integrated over such relatively short times. If one ignores this aspect, and simply considers sensitivity to be a measure of the amount of material one can detect over background in either method, the radioactive method clearly has higher sensitivity. The most sensitive of the four dyes we are using is fluorescein, and when small amounts of fluorescein-labelled primers are detected during electrophoresis on short tube gels, we obtain a minimum detectable level (defined here as a signal-to-noise ratio of 1) of ~10 amol (1 amol is 10^{-18} mol). Approximate minimum detectable levels obtained for the other dyes are NBD, 40 amol; tetramethylrhodamine, 20 amol; and Texas Red, 50 amol. These levels are about one order of magnitude less sensitive than those typically obtained with autoradiography⁷. The sensitivity of this method could be increased in several ways (see discussion below), which would be of value for extending the amount of sequence information obtained in a run and increasing the accuracy of the analysis.

Future directions

Here we have demonstrated the practicality of a novel method for the automated non-isotopic sequence analysis of DNA. This work opens up several avenues for further investigation. First, the fluorescence sequencing method that we have described will benefit from optimization of several interacting factors, including (1) the gel itself, including its length, diameter and composition (for example, different acrylamide percentages, gradients), (2) the procedures and reagents used in the sequencing reactions, (3) the electrophoresis conditions (for example, voltage, current and temperature), (4) the optics and electronics used in data acquisition, (5) the chemistry used in fluorescent primer synthesis (for example, attaching multiple dye molecules per primer to increase sensitivity, adding linker arms to the dyes to compensate for their non-identical electrophoretic mobilities, finding

new dyes with improved fluorescence characteristics), and (6) the software used in data reduction. We have obtained resolved peaks with good signal-to-noise 400 bases into the sequence in some instances, even with the present relatively unoptimized configuration. It is therefore reasonable to expect that an optimized system would yield sequence information beyond position 500 on a routine basis.

The data analysis methods we have developed to date reduce the raw data into a form which is interpretable by the user. We are presently developing the software to perform the final step of data analysis, the interpretative step of assigning the DNA sequence to the data. This interpretation must take into account the high degree of variability in peak intensity obtained in the enzymatic sequencing reactions (see Fig. 4b, particularly the Texas Red-C (Tex-C) reaction), and the possibility of 'false' peaks (see, for example, the false C peaks at base numbers 43, 87 and 116 in Fig. 4b). The software will be able to minimize, but not to eliminate, these problems. It is therefore important that bases which cannot be assigned unambiguously are left unidentified, and that the sequence of unknown DNAs is determined on both strands. A reasonable goal for the system accuracy is a 1% error rate for a single strand, which would give a 0.01% error rate or 1 base in 10,000 for the sequence determined from both strands. This level of accuracy is satisfactory for most applications, and is comparable to or better than the accuracies generally obtained in DNA sequence analysis by conventional methods.

It will also be of great value to apply this fluorescence technology to the chemical method of DNA sequence analysis. This is important for several reasons. First, as mentioned previously, there are occasionally regions of DNA that are difficult to sequence by the enzymatic method but which are usually amenable to analysis by the chemical method. Second, whereas the enzymatic method is characterized by significant peak-to-peak variations in intensity, visible in both autoradiograms and in the fluorescence data presented here, the chemical method generates a much more uniform distribution of fragments of different lengths, which would facilitate data analysis. Third, the simple and inexpensive reagents used in the chemical method can be stored easily, and are easier to handle in a machine for automating the sequencing reactions than the delicate reagents (for example, the Klenow fragment of DNA polymerase) used in the enzymatic reactions. Recent advances in solid-phase methods of sequence analysis by the chemical method^{8,9} will also be of great value in automating those reactions.

Thus, the practicality of a novel non-isotopic method for automated DNA sequence analysis has been demonstrated. It is our hope that this work will help to eliminate much of the labour associated with the structural analysis of DNA, and thereby allow investigators to focus on the more interesting and important questions of modern biology.

We thank Dr Walter Craig for invaluable advice on the mathematics used in data analysis as well as for critical reading of the manuscript; Dr Steven Fung for helpful advice and discussion; Mr Mike Walsh and Mr Tim Heitzman for technical support in the design and construction of the filter wheel assemblies, as well as much invaluable assistance with hardware; and Mr Frank Ostrander for help in the construction of the instrumentation. The concept of using four different dyes was conceived in conjunction with Mr Tim Hunkapiller of Caltech and Dr Michael Hunkapiller of Applied Biosystems. This research was supported by NSF grant DMB-8500298, the Baxter Foundation, Monsanto Chemical Co. and Upjohn, Inc. L.M.S. was a NIH postdoctoral trainee (HD07257) during part of the work described here.

Received 30 December 1985; accepted 11 April 1986.

1. Sanger, F., Nicklen, S. & Coulson, A. R. *Proc. natn. Acad. Sci. U.S.A.* **74**, 5463–5467 (1977).
2. Smith, A. J. H. *Meth. Enzym.* **65**, 560–580 (1980).
3. Maxam, A. M. & Gilbert, W. *Meth. Enzym.* **65**, 499–559 (1980).

4. Smith, L. M., Fung, S., Hunkapiller, M. W., Hunkapiller, T. J. & Hood, L. E. *Nucleic Acids Res.* 13, 2399–2412 (1985).
 5. Smith, L. M., Kaiser, R. J., Sanders, J. Z. & Hood, L. E. *Meth. Enzym.* (in the press).
 6. Atkinson, T. & Smith, M. *Oligonucleotide Synthesis: A Practical Approach* (ed. Gait, M. J.) 35–81 (IRL, Oxford, 1984).
7. Forster, A. C., McInnes, J. L., Skingle, D. C. & Symons, R. H. *Nucleic Acids Res.* 13, 745–761 (1985).
 8. Chuvpilo, S. A. & Kravchenko, V. V. *Sov. J. bioorg. Chem.* 9, 1694–1697 (1983).
 9. Rosenthal, A., Schwertner, S., Hahn, V. & Hunger, H. *Nucleic Acids Res.* 13, 1173–1184 (1985).

LETTERS TO NATURE

Coordinated Exosat and spectroscopic observations of flare stars and coronal heating

C. J. Butler*, M. Rodono†, B. H. Foing‡ & B. M. Haisch§

* Armagh Observatory, College Hill, Armagh BT61 9DG, UK

† Institute of Astronomy, University of Catania, Italy

‡ European Southern Observatory, Santiago, Chile

§ Lockheed Palo Alto Research Laboratory, Palo Alto, California 94304, USA

The X-ray flux of dMe stars is thought to arise from two distinct mechanisms, one involving a continuous ‘quiescent’ emission from a high-temperature plasma and the other involving the dramatic flare events which have long been known to occur on these stars. We present here some results of simultaneous monitoring of the two flare stars, UV Ceti and EQ Peg, with Exosat and ground-based optical spectroscopy. We observe short-timescale variability in the 0.1–2-keV emission from both these objects and, in the case of UV Ceti, find a strong correlation between the soft X-ray and H γ fluctuations. The implication is that much of the low-level X-ray flux previously considered ‘quiescent’ probably originates from small flare events.

Our understanding of coronal structure and of mechanisms for coronal heating in the Sun and stars has evolved considerably as a result of the solar observations of Skylab and the Solar Maximum Mission (SMM) and the stellar observations of the Einstein Observatory and now Exosat. The Skylab photographs of the Sun showed that the soft X-ray emission originated almost exclusively in active-region loops, in larger loops connecting active regions and in X-ray bright points, which are thought to be unresolved, small-scale loops of newly emerging magnetic flux. In place of the diffuse Parker-type hot corona/wind, the

closed magnetic loop is now widely thought of as the basic unit of coronal structure^{1–3}. By contrast, regions of open magnetic field, called coronal holes, are dark in X rays and appear to be the primary source of the solar wind. Because many of the Skylab and other images emphasize the higher-temperature and more dense structures (the emission for a collisionally excited line is $\sim n(e)^2$), it may well be that there is a significant diffused coronal component, in addition to coronal loops and coronal holes. Whether or not this is the case, the concept of a ‘quiet corona’ (be it diffuse or the average state of the quasi-steady loop ensemble) has persisted since the discovery of the solar corona. This concept has recently been extended to ‘quiet stellar coronae’⁴, the dichotomy being one between the quasi-steady evolution of high-temperature, X-ray-emitting structures, on timescales of hours to days to weeks, and the more obvious variability associated with flares. The heating of the ‘quiet corona’ and the nature and energetics of solar flares have thus historically been viewed as different and distinct problems.

However, recently, using balloon-borne instrumentation, a significant number of solar hard X-ray microflares have been observed⁵, presumably produced by bremsstrahlung of non-thermal electron beams in the solar chromosphere and transition region. It was found that the average rate of energy deposition above 20 keV and above the detection threshold amounted to $\sim 10^{24}$ erg s⁻¹. In addition, the integral number of events appeared to vary as the inverse of the peak flux down to their detection threshold, in which case the total rate of energy release, allowing for low-level events, could begin to approach the total quiescent solar coronal X-ray luminosity⁶, $L_x = 5 \times 10^{27}$ erg s⁻¹. The timescales for these microflares ranged from seconds to tens of seconds in duration. Elsewhere in the spectrum, short-lived extreme-ultraviolet bursts of subflare magnitude have been observed on the Sun in several transition-region lines; these bursts probably result from the same electron beaming event that creates the hard X-rays⁷. From a re-analysis of Skylab data⁸, frequent subflare-like extreme-ultraviolet brightenings have been found near the foot-points of loops, and using the SMM

Fig. 1 Soft X-ray flux detected by the CMA on Exosat from UV Ceti, compared with the H γ peak intensity from the ESO 3.6-m telescope. *a*, X-rays (LE), bin size 30 s; *b*, X-rays (LE), bin size 60 s; *c*, H γ peak, exposure 60 s.

